

Explicit Interaction Network for Aspect Sentiment Triplet Extraction

Peiyi Wang, Tianyu Liu, Damai Dai, Runxin Xu, Baobao Chang, Zhifang Sui
 MOE Key Lab of Computational Linguistics, Peking University, Beijing, 100871, China
 {wangpeiyi9979, runxinxu}@gmail.com
 {daidamai, tianyu0421, chbb, szf}@pku.edu.cn

Abstract—Aspect Sentiment Triplet Extraction (ASTE) aims to recognize targets, their sentiment polarities and opinions explaining the sentiment from a sentence. ASTE could be naturally divided into 3 atom subtasks, namely target detection, opinion detection and sentiment classification. We argue that the proper subtask combination, compositional feature extraction for target-opinion pairs, and interaction between subtasks would be the key to success. Prior work, however, may fail on ‘one-to-many’ or ‘many-to-one’ situations, or derive non-existent sentiment triplets due to defective subtask formulation, sub-optimal feature representation or the lack of subtask interaction. In this paper, we divide ASTE into target-opinion joint detection and sentiment classification subtasks, which is in line with human cognition, and correspondingly utilize sequence encoder and table encoder to handle them. Table encoder extracts sentiment at token-pair level, so that the compositional feature between targets and opinions can be easily captured. To establish explicit interaction between subtasks, we utilize the table representation to guide the sequence encoding, and inject the sequence features back into the table encoder. Experiments show that our model outperforms state-of-the-art methods on six popular ASTE datasets.

Index Terms—Aspect sentiment triplet extraction, compositional feature, explicit interaction, subtask combination.

I. INTRODUCTION

ASPECT sentiment analysis [1] aims to identify the sentiment polarity, e.g., *positive*, *neutral* and *negative*, for the specific target in the given context. Taking one step forward, Aspect Sentiment Triplet Extraction (ASTE) [2] is a recently proposed sentiment analysis task that extracts sentiment triplet including target entity, its sentiment polarity and, more importantly, opinion span which rationalizes the extracted sentiment. As shown in Figure 1, we utilize the blue and green boxes to represent the targets (e.g., *sofa*) and corresponding opinions (e.g., *nice*). In this way, we can obtain two triplets (*sofa*, POS, *nice*) and (*sofa*, NEG, *expensive*) from S_1 .

As ASTE is a composite triplet extraction task, prior work divides the task into different components. As illustrated in Figure 2, we summarize 3 atom subtasks, namely target detection (T), opinion detection (O) and sentiment classification (S) and figure out different subtask combinations for four mainstream baselines. In Figure 2(a), Peng20 [2] proposes a two-stage model, which combines target detection and sentiment classification (TS) and separately models target-polarity tuple and corresponding opinion, followed by a binary matching classifier. In Figure 2(b), JET [3] combines all 3 atom

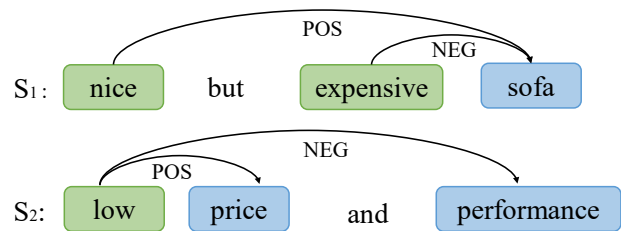


Fig. 1: Two examples of ASTE. POS, NEU and NEG are short for positive, neutral and negative.

subtasks (OTS) by formulating ASTE as a sequence labeling task, and develops a composite tag system that consists of target, opinion and sentiment for each token. Moreover, in Figure 2(c), OTE [4] separately models the 3 atom subtasks by a multi-task learning framework. Lastly in Figure 2(d), GTS [5] aggregates all 3 atom subtasks (OTS) by formulating ASTE as a grid tagging problem.

We argue that a reasonable subtask combination and effective interaction between subtasks would be fundamental to the success of ASTE. The binding between a specific target and a unique sentiment, e.g., Peng20 and JET (Figure 2(a) and (b)), would fail in the ‘many-to-one’ situations like S_1 in Figure 1, in which the target ‘sofa’ has two related sentiments: POS for ‘nice sofa’ and NEG for ‘expensive sofa’. GTS (Figure 2(d)) improves JET (Figure 2(b)) by mitigating the confusions in ‘many-to-one’ situations with a grid tagging formulation, however both GTS and JET try to aggregate the three atom subtask into a unified model. The simple aggregation, as verified by our experiments, is sub-optimal in terms of subtask combination. Inspired by human cognition, i.e., judging sentiment based on both target and opinion (e.g., ‘nice sofa’ and ‘expensive sofa’), we formulate ASTE as two components: the joint target-opinion detection, and sentiment classification as shown in Figure 2(e). Furthermore, as the extracted targets, opinions and sentiments are highly interdependent, we posit effective interaction between subtasks would enhance the model performance on ASTE. With independent modeling of each subtask like OTE (Figure 2(c)), the subtasks have no interaction except the shared sentence (base) encoder, which we call implicit interaction. Implicit interaction can only be successful under the assumption that the base encoder is sufficient to capture the correlation among subtasks. On the contrary, explicit interaction network on the top of the base encoder could

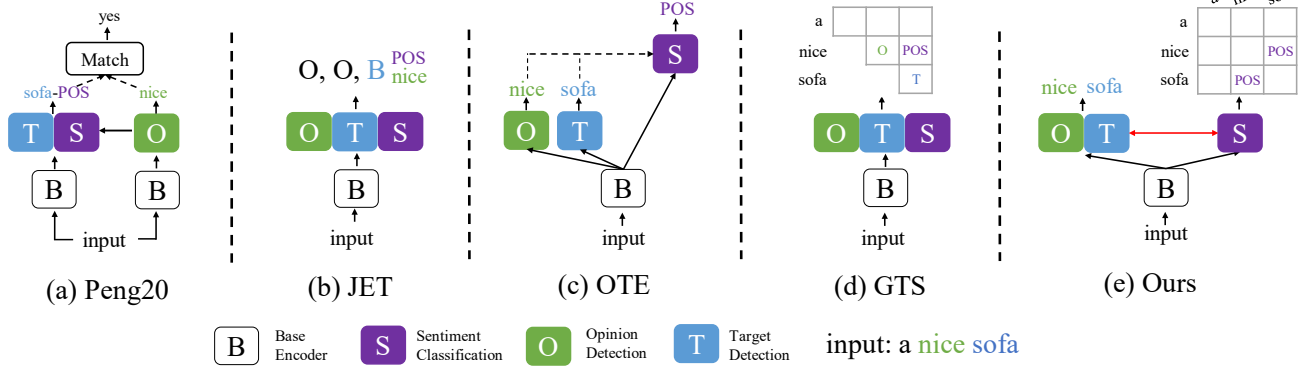


Fig. 2: Illustration of different subtask combinations in ASTE. We elaborate the detailed subtask settings of three mainstream baseline models in the second paragraph of Section I. Figure (e) depicts the proposed model, we formulate ASTE as two components: target-opinion joint detection and sentiment classification, and also build bidirectional explicit interaction between the two components.

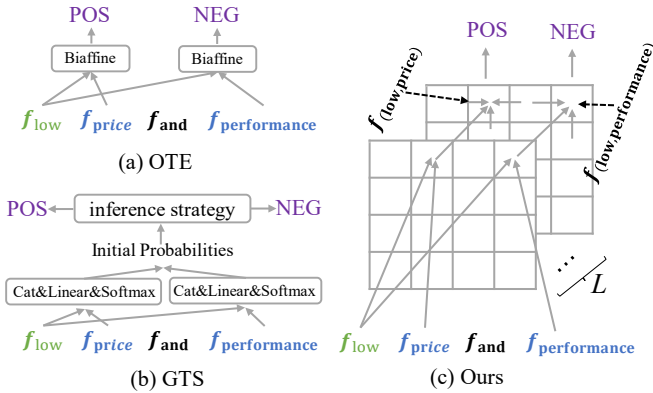


Fig. 3: Illustration of sentiment classification for different models. OTE and GTS predict sentiment by token level features. However, our model first extracts token-pair level features, and then performs sentiment classification based on these features.

establish more profound communications between subtasks [2], [6], [7]. Although prior work like Peng20 (Figure 2(a)) also utilized inter-task interaction, it is unidirectional from opinion detection to joint target-sentiment extraction thus the acquisition of opinion would be somewhat blind without knowing the target. We instead use a bidirectional explicit interaction between target-opinion joint detection and sentiment classification.

Most of the previous methods only extract token-level sentiment features, which ignore the compositional features of target-opinion pairs. Taking the S_2 in Figure 1 as an example, the prior works usually encode the sentence ‘low price and performance’ by a sequence encoder and then obtain the token-level sentiment features, e.g. $f(\text{low})$, $f(\text{price})$, $f(\text{and})$, $f(\text{performance})$ ($f(x)$ represents the sentiment feature of word x). Then different sentiment classifiers are built upon the extracted token-level features. As shown in Figure 3, OTE exploited a rather simple sentiment classifier (biaffine scorer [8]) while GTS proposed a more sophisticated one, i.e. grid inference over feature extractor. Both of them use the same opinion feature $f(\text{low})$ to predict the sentiment

polarities for different target-opinion pairs. Since the opinion word ‘low’ indicates different sentiment polarities when paired with different targets like ‘price’ and ‘performance’ in S_2 , the models with only token-level features tend to make wrong predictions, e.g., (low, NEG, price) or (low, POS, performance). We instead utilize a table encoder (Figure 3(c)), which extracts pairwise sentiment features for each unique target-opinion pair, e.g. $f(\text{low}, \text{price})$, $f(\text{low}, \text{performance})$, and then accordingly predict the sentiment polarities with the compositional features. We find in our experiments that the compositional feature extractor greatly boosts the performance of ASTE, especially in more complex conditions where multiple sentiment triplets exist in the same sentence.

Specifically we formulate the target-opinion joint detection as sequence labeling to identify both target and opinion tokens with a sequence encoder, and we also adopt a two-dimensional (2D) table encoder for sentiment classification, along with two explicit interaction mechanisms between table and sequence encoders. The 2D table encoder could effectively model token-pair features with compositional representations. It would ease the difficulties in the ‘many-opinions-to-one-target’ and ‘one-opinion-to-many-targets’ challenges shown in Figure 1, and reduce the erroneous predictions on non-existent triplets, which is observed in case studies. To build explicit interaction between table and sequence encoders, we use table guide attention (TGA) which guides the self-attention in sequence encoder with table representation, and sequence feature injection (SFI) which in turn enhances table representation with features from target-opinion joint labeling. We summarize our contributions as follows:

- We formulate ASTE as target-opinion joint detection and sentiment classification, which is in line with human cognition, and utilize bidirectional explicit interaction between the two subtasks with table guide attention (TGA) and sequence information injection (SFI).
- Table encoder is better at identifying different sentiments for divergent target-opinion combinations by compositional token-pair representations, which greatly reduces

errors in predictions.

- Extensive experiments on the benchmark datasets show that our model achieves new state-of-the-art performance on six popular ASTE datasets.

II. RELATED WORK

A. Aspect-based Sentiment Analysis

Sentiment Analysis is widely used in actual scenarios [27], [28]. There are many variants of sentiment analysis. In terms of task granularity, it can be divided into document level sentiment analysis [29], [30], [31] and aspect level sentiment analysis [32], [17], [33]. Among all variant of sentiment analysis, the most closely related to the ASTE problem is the Aspect-based sentiment analysis (ABSA). ABSA proposed by [34] refers to addressing various sentiment analysis tasks based on specific target words. The most widely known form of ABSA is aspect sentiment classification [35], [36], which aims to predict the sentiment polarity of a given aspect. The model used for the ABSA task usually enhances the interaction between the aspect and the context as much as possible [37], [25], so that the model can pay attention to fine-grained sentiment changes and improve the performance. While Aspect term extract (ATE) [38], [39], [40] requires a model to detect targets from a sentence. ATE is usually treated as sequence labeling problem and solved by CRF-based approaches. Aspect-sentiment pair extraction (ASPE) aims to detect targets and to classifies the sentiment of them [41], [20]. On the top of ATE and ASPE, ASTE extracts the discussed targets, the sentiment of targets, and the opinions explaining why the targets have such sentiment polarities. Compared with ASPE, ASTE can give reasons for sentiment classification, so it is more interpretable. In parallel with our work, [15] inserts four special tags into sentence to guide the encoder to extract compositional feature. [13] uses the machine reading comprehension framework, and propose a query such as ‘whats the sentiment polarity of [price] and [low]’ to classify the sentiment. Both of them try to utilize pairwise compositional features in the sentiment prediction with the specialized templates (input sequences or questions), which are fundamentally different from the proposed table encoder with explicit interaction.

B. Joint Entity and Relation Extraction

Joint Entity and Relation Extraction (JERE) aims to extract triplets, consisting of named entities and their relations from the sentence, which is similar to ASTE in the form. Many methods have been proposed to solve JERE, such as pipeline extraction methods [42], joint extraction methods [9], [10], [7] and generative methods [43], [44], [45]. Our method is similar to [7] in JERE, which also extracts triplets from sentence through sequence and table encoders. However, our method is different from [7] from both motivation and model designing perspectives: 1) The core contribution of this paper is on the model architecture side of ASTE. We summarize the model architectures of previous work and figure out their potential weakness on defective subtask combination and lack of interaction among subtasks. We thus prove that proper subtask combination and bidirectional interaction among

subtasks are the key to successfully from ASTE, which provides actionable insights to NLP community and is different from cfrom the motivation perspective. 2) From model designing perspective, although the model structure is largely inspired by [7], we first point out the importance of the token-pair level feature for ASTE, thus we utilize a table encoder with Multi-Dimension Gated Recurrent Unit (MDGRU) [7], [11], [12] to model it. Note that We do NOT take the credit of designing table encoder. Other encoders, e.g., Transformer [26] (each input corresponds to a token-pair), can also serve the token-pair level feature extractor. In addition, our table encoder also adopt different table filling method, i.e. we use symmetric matrix for table filling while the table in [7] is asymmetric (relation type is directional). At last, the sequence encoder we use is a basic GRU while [7] used a dedicated Transformer variant as basic building block.

III. METHODOLOGY

A. Task Formulation

Formally, in ASTE, given an input sentence $w = [w_i]_{1 \leq i \leq N}$, where each w_i represents a token in the sentence. We need to extract all triplets $\{(t_k, s_k, o_k)\}_{k=1}^K$, where $t_k = w_{a:b}$ is a target, $s_k \in \{\text{POS}, \text{NEG}, \text{NEU}\}$ is the sentiment of t_k , and $o_k = w_{c:d}$ is an opinion explaining s_k , $w_{m:n}$ denotes a span in w with indices from m to n .

We split ASTE into target-opinion detection and sentiment classification. In the target-opinion detection, we need to extract all potential targets $\{t_i\}_{i=1}^T$ and opinions $\{o_j\}_{j=1}^O$ from the sentence. We solve this subtask via sequence labeling, where the golden tags are the standard BIO scheme.¹

In the sentiment classification, we need to decide the sentiment of token pairs. We regard this subtask as a table filling problem [9], [10], [7], [4]. Specially, for a sentence including N tokens, we create a sentiment table T^s with the shape $N \times N$. An example of table filling is shown in the top-right part of Figure 4(a). Formally, for a sentence with triplets $\{(t_k, s_k, o_k)\}_{k=1}^K$, the table cell (m, n) has label $T_{m,n}^s = s_k$ if $m, n \in C_{t_k, o_k}$,

$$C_{t_k, o_k} = \{(m, n) | m \in [a, b] \wedge n \in [c, d] \vee m \in [c, d] \wedge n \in [a, b]\} \quad (1)$$

where $t_k = w_{a:b}$, $o_k = w_{c:d}$, otherwise, $T_{m,n}^s = \text{N/A}$, which indicates that token i and token j have no sentiment relationship. There are four kinds of labels for table cells, $\{\text{N/A}, \text{POS}, \text{NEG}, \text{NEU}\}$.

B. Model Overview

We propose a model that jointly performs target-opinion detection and sentiment classification. As shown in Figure 4(a), we use a shared base encoder to extract shared features for two subtasks, and a multi-layer sequence encoder for target and opinion detection. Meanwhile, a multi-layer 2D table encoder is utilized to predict the sentiment of token pairs. We also adopt a bidirectional explicit interaction between two encoders.

¹{O, B-Target, B-Opinion, I-Target, I-Opinion}.

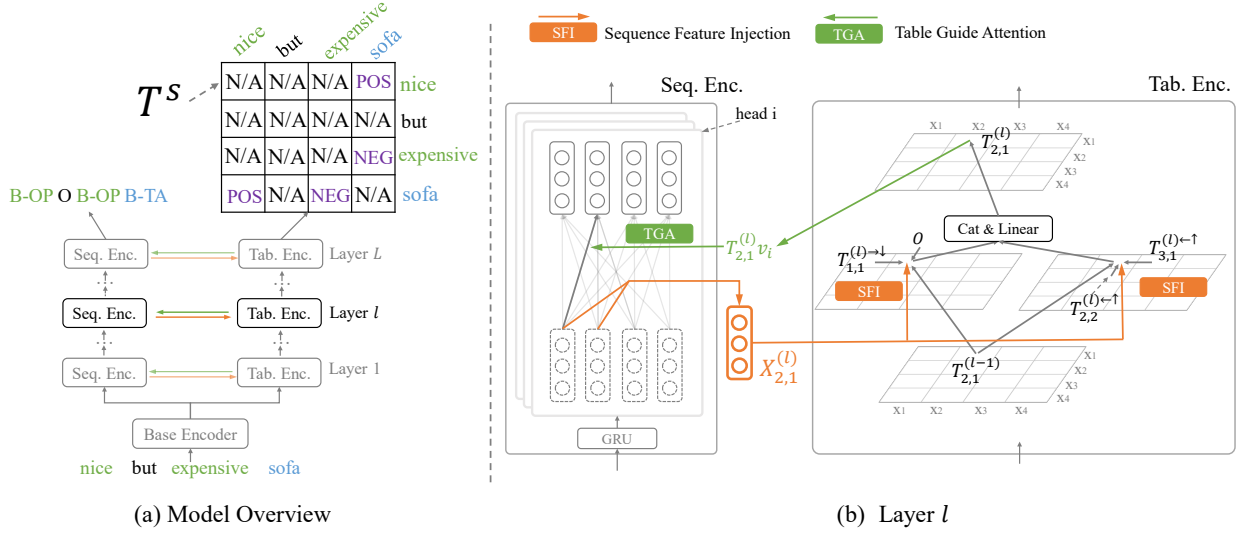


Fig. 4: (a) Model Overview: The left part is a multi-layer sequence encoder detecting targets and opinions by sequence labeling, OP and TA represent Opinion and Target, respectively. The right part is a multi-layer table encoder performing sentiment classification via table filling. The green and orange arrows denote two explicit interaction mechanisms. (b) Illustration of the l -th layer of our model. The right part is the table encoder consisting of two MD-GRUs with the input X_l generated by the sequence feature injection. The left part is the sequence encoder with a GRU followed by a feature aggregation through the table guide attention.

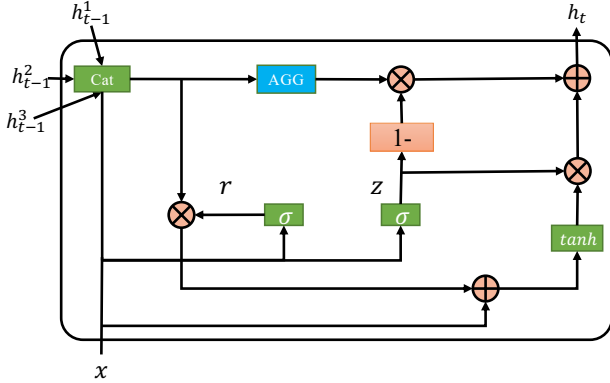


Fig. 5: The internal structure of MDGRU, which takes three hidden states from last time step and aggregate hidden states by a special gate mechanism.

C. Shared Base Encoder

To build the implicit interaction between two encoders, given a sentence $w = [w_i]_{1 \leq i \leq N}$, we first encode each token w_i to $\mathbf{x}_i \in \mathbb{R}^{d_w}$ by an embedding layer, e.g. GloVe or BERT, where d_w is the embedding dimension. Then we get the shared representation for the subsequent two subtasks,

$$\mathbf{B} = \mathbf{X}\mathbf{W}_b + \mathbf{b}_b \quad (2)$$

where $\mathbf{W}_b \in \mathbb{R}^{d_w \times d_h}$ and $\mathbf{b}_b \in \mathbb{R}^{d_h}$ are trainable parameters.

D. Table Encoder

a) *Multi-Dimension Gated Recurrent Unit*: To extract the compositional feature, we build our table encoder via **Multi-Dimension Gated Recurrent Unit (MDGRU)** following [7]

that combines the multi-dimension recurrent neural network [11] and the Gated Recurrent Unit (GRU) [12]. With an input $\mathbf{x} \in \mathbb{R}^{d_h}$, compared with GRU, MDGRU can accept three hidden states from the previous time step, $\mathbf{h}_{t-1}^1, \mathbf{h}_{t-1}^2, \mathbf{h}_{t-1}^3$, and get the hidden state at the current time step \mathbf{h}_t as follows,

$$\mathbf{h}_t = \text{MDGRU}(\mathbf{x}, \mathbf{h}_{t-1}^1, \mathbf{h}_{t-1}^2, \mathbf{h}_{t-1}^3) \quad (3)$$

where $\mathbf{h}_t, \mathbf{h}_{t-1}^1, \mathbf{h}_{t-1}^2, \mathbf{h}_{t-1}^3 \in \mathbb{R}^{d_h}$. In detail, as shown in Figure 5, MDGRU first concatenates three previous hidden states to form a comprehensive previous hidden state $\tilde{\mathbf{h}}_{t-1} = [\mathbf{h}_{t-1}^1; \mathbf{h}_{t-1}^2; \mathbf{h}_{t-1}^3] \in \mathbb{R}^{3d_h}$, and then calculates the reset gate \mathbf{r} and update gate \mathbf{z} as follows,

$$\mathbf{r} = \sigma([\mathbf{x}; \tilde{\mathbf{h}}_{t-1}]\mathbf{W}^r + \mathbf{b}^r) \quad (4)$$

$$\mathbf{z} = \sigma([\mathbf{x}; \tilde{\mathbf{h}}_{t-1}]\mathbf{W}^z + \mathbf{b}^z) \quad (5)$$

where $\mathbf{W}^r, \mathbf{W}^z \in \mathbb{R}^{4d_h \times d_h}$ and $\mathbf{b}^r, \mathbf{b}^z \in \mathbb{R}^{d_h}$ are trainable parameters, and σ is the sigmoid function. Finally it gets the candidate hidden state $\tilde{\mathbf{h}} \in \mathbb{R}^{d_h}$ and output hidden state $\mathbf{h}^t \in \mathbb{R}^{d_h}$,

$$\tilde{\mathbf{h}} = \tanh(\mathbf{x}\mathbf{W}^x + \mathbf{r} \odot (\tilde{\mathbf{h}}_{t-1}\mathbf{W}^p) + \mathbf{b}^h) \quad (6)$$

$$\mathbf{h}^t = \mathbf{z} \odot \tilde{\mathbf{h}} + (1 - \mathbf{z}) \odot \tilde{\mathbf{h}}_{t-1} \quad (7)$$

where $\mathbf{W}^x \in \mathbb{R}^{d_h \times d_h}$, $\mathbf{W}^p \in \mathbb{R}^{3d_h \times d_h}$ and $\mathbf{b}^h \in \mathbb{R}^{d_h}$ are trainable parameters, \odot is the element-wise product, and $\tilde{\mathbf{h}}_{t-1}$ is aggregated through a gate mechanism with $\mathbf{h}_{t-1}^1, \mathbf{h}_{t-1}^2$ and \mathbf{h}_{t-1}^3 as inputs,

$$\tilde{\mathbf{h}}_{t-1} = \sum_{i=1}^3 \lambda_i \odot \mathbf{h}_{t-1}^i \quad (8)$$

where $\lambda_1, \lambda_2, \lambda_3 \in \mathbb{R}^{d_h}$ are weight gates calculated by:

$$\begin{aligned} \lambda_1, \lambda_2, \lambda_3 &= \text{softmax}(\tilde{\lambda}_1, \tilde{\lambda}_2, \tilde{\lambda}_3) \\ \tilde{\lambda}_m &= [\mathbf{x}; \mathbf{h}_{t-1}] \mathbf{W}_m^\lambda + \mathbf{b}_m^\lambda \end{aligned} \quad (9)$$

where $\mathbf{W}_m^\lambda \in \mathbb{R}^{4d_h \times d_h}$, $\mathbf{b}_m^\lambda \in \mathbb{R}^{d_h}$ are trainable parameters. In this way, each hidden state of GRU can represent a token pair on the table.

b) *Table Encoder*: To better handle the divergent sentiment situation and reduce the erroneous predictions on non-existent triplets, we use a multi-layer 2D table encoder whose each cell corresponds to a token pair, to generate sentiment features at the token-pair level. For the cell (m, n) at layer (l) , as shown in the right part of Figure 4(b), the table encoder uses two MDGRUs to receive features from the previous layer, the sequence encoder, and different directions around the cell. With these features, the table encoder updates its states as follows,

$$\mathbf{T}_{m,n}^{(l)} = [\mathbf{T}_{m,n}^{(l) \rightarrow \downarrow}; \mathbf{T}_{m,n}^{(l) \leftarrow \uparrow}] \mathbf{W}_t^{(l)} + \mathbf{b}_t^{(l)} \quad (10)$$

$$\mathbf{T}_{m,n}^{(l) \rightarrow \downarrow} = \text{MDGRU}_1^{(l)}(\mathbf{X}_{m,n}^{(l)}, \mathbf{T}_{m,n}^{(l-1)}, \mathbf{T}_{m-1,n}^{(l) \rightarrow \downarrow}, \mathbf{T}_{m,n-1}^{(l) \rightarrow \downarrow}) \quad (11)$$

$$\mathbf{T}_{m,n}^{(l) \leftarrow \uparrow} = \text{MDGRU}_2^{(l)}(\mathbf{X}_{m,n}^{(l)}, \mathbf{T}_{m,n}^{(l-1)}, \mathbf{T}_{m+1,n}^{(l) \leftarrow \uparrow}, \mathbf{T}_{m,n+1}^{(l) \leftarrow \uparrow}) \quad (12)$$

where $\mathbf{W}_t^{(l)} \in \mathbb{R}^{2d_h \times d_h}$ and $\mathbf{b}_t^{(l)} \in \mathbb{R}^{d_h}$ are trainable parameters. $[\cdot]$ means the concatenation operation, $\mathbf{T}_{m,n}^{(l-1)}$ is the vector of the table encoder cell (m, n) at layer $(l-1)$, $\mathbf{X}_{m,n}^{(l)}$ is generated from the sequence encoder, which will be introduced in Section III-F. $\mathbf{T}^{(l) \rightarrow \downarrow}$ and $\mathbf{T}^{(l) \leftarrow \uparrow}$ are hidden states of two MDGRUs, and we pad them with an all-zero vector $\mathbf{0}$ when the index is out of boundary. For the first layer, we represent the $\mathbf{T}_{m,n}^{(0)}$ by combining the representations of corresponding token pair,

$$\mathbf{T}_{m,n}^{(0)} = \text{ReLU}([\mathbf{B}_m; \mathbf{B}_n] \mathbf{W}_t^{(0)} + \mathbf{b}_t^{(0)}) \quad (13)$$

where $\mathbf{W}_t^{(0)} \in \mathbb{R}^{2d_h \times d_h}$ and $\mathbf{b}_t^{(0)} \in \mathbb{R}^{d_h}$ are trainable parameters. \mathbf{B} is the output of our base encoder.

E. Table Guided Sequence Encoder

Since two subtasks are highly interdependent, some features in the table encoder can promote the target-opinion detection. We provide the sequence encoder with the features from the table encoder. Specially, we use a multi-layer table guided sequence encoder. As shown in the left part of Figure 4(b), at layer (l) , the sequence encoder first encodes the features from the previous layer or the base encoder through GRU,

$$\mathbf{S}^{(l)} = \begin{cases} \text{GRU}^{(l)}(\mathbf{B}) & l = 1 \\ \text{GRU}^{(l)}(\mathbf{S}^{(l-1)}) & l > 1 \end{cases} \quad (14)$$

where $\mathbf{S}^{(l-1)}$ is the output of the previous sequence encoder layer. Then, since each cell of the table encoder corresponds a token pair, motivated by [7], we use Table Guide Attention (TGA) (the green arrow in Figure 4(b)) to aggregate $\mathbf{S}^{(l)}$ as follows,

$$\mathbf{S}^{(l)} = [\text{head}_1; \dots; \text{head}_h] \mathbf{W}_o \quad (15)$$

$$\text{head}_i = \text{softmax}\left(\frac{\mathbf{T}^{(l)} \mathbf{v}_i}{\sqrt{d_h}}\right) \mathbf{S}^{(l)} \mathbf{W}_i \quad (16)$$

where i denotes the i -th head in TGA, h is the number of heads, $\mathbf{T}^{(l)} \in \mathbb{R}^{N \times N \times d_h}$ is the hidden state of the table encoder at layer (l) . The $\mathbf{W}_o \in \mathbb{R}^{d_h \times d_h}$, $\mathbf{v}_i \in \mathbb{R}^{d_h}$ and $\mathbf{W}_i \in \mathbb{R}^{d_h \times \frac{d_h}{h}}$ are trainable parameters, and we omit their superscripts (l) for clarity.

F. Sequence Feature Injection

Because the table encoder predicts the token pairs' sentiment that is generated from the sentiment of target-opinion pairs, some features used to predict targets and opinions can also be used in the table encoder. We thus utilize Sequence Feature Injection (SFI) to bring some helpful features in the sequence encoding process into the table encoder.

As shown in the orange arrow of Figure 4(b), we provide each table cell (m, n) with the feature from corresponding token pair in the sequence encoder as follows,

$$\mathbf{X}_{m,n}^{(l)} = \text{ReLU}([\mathbf{S}_m^{(l)}; \mathbf{S}_n^{(l)}] \mathbf{W}_s^{(l)} + \mathbf{b}_s^{(l)}) \quad (17)$$

where $\mathbf{W}_s^{(l)} \in \mathbb{R}^{2d_h \times d_h}$, $\mathbf{b}_s^{(l)} \in \mathbb{R}^{d_h}$ are trainable parameters, and $\mathbf{X}_{m,n}^{(l)}$ is the input of Equation 11 and Equation 12.

G. Training and Inference

For an input sentence $\mathbf{w} = [w_i]_{1 \leq i \leq N}$, in the target-opinion detection, we utilize the output of the L -th layer sequence encoder to predict BIO tags,

$$P(y_i | \mathbf{S}_i^{(L)}) = \text{softmax}(\mathbf{S}_i^{(L)} \mathbf{W}_1 + \mathbf{b}_1) \quad (18)$$

where $\mathbf{W}_1 \in \mathbb{R}^{d_h \times 5}$ and $\mathbf{b}_1 \in \mathbb{R}^5$ are trainable parameters, and we use cross-entropy as the loss function,

$$\mathcal{L}_{seq} = - \sum_{i=1}^N \log P(y_i^* | \mathbf{S}_i^{(L)}) \quad (19)$$

where y_i^* is the golden BIO tag of token x_i . Meanwhile, the sentiment of token pairs is determined by the output of the L -th layer table encoder,

$$P(y_{m,n} | \mathbf{T}_{m,n}^{(L)}) = \text{softmax}(\mathbf{T}_{m,n}^{(L)} \mathbf{W}_2 + \mathbf{b}_2) \quad (20)$$

where $\mathbf{W}_2 \in \mathbb{R}^{d_h \times 4}$ and $\mathbf{b}_2 \in \mathbb{R}^4$, and the loss function of this subtask is also cross-entropy,

$$\mathcal{L}_{table} = - \sum_{m=1}^N \sum_{n=1}^N \log P(y_{m,n}^* | \mathbf{T}_{m,n}^{(L)}) \quad (21)$$

where $y_{m,n}^*$ is the golden sentiment of the cell (m, n) . The final loss is $\mathcal{L} = \mathcal{L}_{seq} + \mathcal{L}_{table}$. For inference, we get the BIO tag of x_i by taking,

$$y_i^* = \arg \max_t P(y_i = t | \mathbf{S}_i^{(L)}) \quad (22)$$

Split	¹⁴ Lap				¹⁴ Rest				¹⁵ Rest				¹⁶ Rest			
	#Sent	#POS	#NEU	#NEG	Sent	#POS	#NEU	#NEG	Sent	#POS	#NEU	#NEG	Sent	#POS	#NEU	#NEG
Train	920	664	117	484	1300	1575	143	427	593	703	25	195	842	933	49	307
Dev	228	207	16	114	323	377	32	115	148	179	9	50	210	225	10	81
Test	339	335	50	105	496	675	45	142	318	291	25	139	320	362	27	76

TABLE I: Statistics of four datasets from ASTE-DATA-V1, #Sent denotes the number of sentences, and #POS, #NEU, #NEG denote the numbers of positive, neutral and negative triplets respectively in dataset

Split	¹⁴ Lap				¹⁴ Rest				¹⁵ Rest				¹⁶ Rest			
	#Sent	#POS	#NEU	#NEG	Sent	#POS	#NEU	#NEG	Sent	#POS	#NEU	#NEG	Sent	#POS	#NEU	#NEG
Train	906	817	126	517	1266	1692	166	480	605	783	25	205	857	1015	50	329
Dev	219	169	36	141	310	404	54	119	148	185	11	53	210	252	11	76
Test	328	364	63	116	492	773	66	155	322	317	25	143	326	407	29	78

TABLE II: Statistics of four datasets from ASTE-DATA-V2.

and detect targets and opinions according to BIO tags of tokens. For each possible target-opinion pair (t_k, o_k) , where $t_k = w_{a:b}$ and $o_k = w_{c:d}$, we predict the sentiment s_k by taking,

$$\arg \max_s \sum_{(m,n) \in C_{t_k, o_k}} P(y_{m,n} = s | \mathbf{T}_{m,n}^{(L)}) \quad (23)$$

where C_{t_k, o_k} is defined by Equation 1.

IV. EXPERIMENTS

A. Datasets and Evaluation Metrics

we evaluate our method on ASTE-DATA-V1² and ASTE-DATA-V2³. ASTE-DATA-V2 refines its previous version ASTE-DATA-V1 by annotating missing triplets. Both of V1 and V2 have four datasets, ¹⁴Rest, ¹⁵Rest, ¹⁶Rest in restaurant domain, and ¹⁴Lap in laptop domain. The details about four datasets of ASTE-DATA-V1 and ASTE-DATA-V2 are included in Table I and Table II, respectively. Moreover, following previous work, e.g., [2], [3], [4], we adopt the precision (P.), recall (R.) and micro F1-measure (F1.) as our evaluation metrics for triplet extraction.

B. Baselines

For systematic comparisons, we introduce a variety of baselines,

- **CMLA+** [2] is modified from CMLA [18]. CMLA use attention mechanism to capture the relationship between words, and extract targets with sentiment together. CMLA+ add an MLP on CMLA to determine whether a triplet is correct in the matching stage.
- **RINANTE+** [2] is modified from RINANTE [19], which uses LSTM-CRF and fuses rules as weak supervision to capture dependency relations of words. The way RINANTE+ determine the correctness of a triplet is the same as CMLA+.
- **Li-unified-R** [2] is modified from [20], which extracts targets, sentiment and opinion spans respectively based

on a multi-layer LSTM neural architecture. The way Li-unified-R determine the correctness of a triplet is the same as CMLA+.

- **Peng20** [2] also decomposes triplet extraction to two stages: extracts unified target-sentiment and opinions via GCN first, then pairs the two results from the results before.
- **JET** [3] regards ASTE as a sequence labeling problem based on unified tags. JET has two variants: JET_t predict the target, the sentiment of target and the corresponding opinion. JET_o predict the opinion, the sentiment of the opinion and the corresponding target.
- **OTE** [4] utilizes a multi-task framework to solve ASTE, which learns joint features of different subtasks via a shared encoder, then predicts targets, opinions by sequence labeling and use a biaffine layer to predict sentiment.
- **GTS** [5] formulates ASTE as an unified grid tagging task. It first extracts sentiment feature of each token, and then get the initial prediction probabilities of toke pairs based on these token-level features. At last, it designs a grid inference strategy to modeling the mutual interactions of all probabilities, and performs the final prediction.
- **S³E²** [16] exploits the syntactic and semantic relationships between the triplet elements with a semantic and syntactic enhanced module.
- **[13]** formulates ASTE as a machine reading comprehension problem, and proposes three types of queries to extract targets, opinions and the sentiment polarities of target-opinion pairs, respectively.
- **Dual-MRC** [21] constructs two machine reading comprehension problems to solve ASTE and other Aspect based sentiment analysis tasks with joint training two BERT-MRC models.
- **[15]** proposes a two-stage model, which first extracts targets and opinions, and then inserts special tags into sentence to identify the specific target-opinion pair and finally predict the sentiment polarity of this pair.
- **[14]** formulates ASTE as a sequence-to-sequence generation problem, and utilizes pre-trained sequence-to-sequence model BART [22] with teacher forcing training to generate targets, opinions and sentiment polarities directly.

²<https://github.com/xuuluuuu/SemEval-Triplet-data/tree/master/ASTE-Data-V1-AAAI2020>

³<https://github.com/xuuluuuu/SemEval-Triplet-data/tree/master/ASTE-Data-V2-EMNLP2020>

(a) Results on ASTE-DATA-V1.

	Models	14Lap			14Rest			15Rest			16Rest		
		<i>P.</i>	<i>R.</i>	<i>F</i> ₁									
GloVe	CMLA+ ‡	31.40	34.60	32.90	40.11	46.63	43.12	34.40	37.60	35.90	43.60	39.80	41.60
	RINANTE+ ‡	23.10	17.60	20.00	31.07	37.63	34.03	29.40	26.90	28.00	27.10	20.50	23.30
	Li-unified-R ‡	42.25	42.78	42.47	41.44	68.79	51.68	43.34	50.73	46.69	38.19	53.47	44.51
	Peng20 ‡	40.40	47.24	43.50	44.18	62.99	51.89	40.97	54.68	46.79	46.76	62.97	53.62
	JET _t ‡	57.98	36.33	44.67	70.39	51.86	59.72	61.99	43.74	51.29	68.99	51.18	58.77
	JET _o ‡	52.01	39.59	44.96	62.26	56.84	59.43	63.25	46.15	53.37	66.58	57.85	61.91
	S ³ E ² ‡	59.43	46.23	52.01	69.08	64.55	66.74	61.06	56.44	58.66	71.08	63.13	66.87
	OTE *	50.52	39.71	44.31	64.68	54.97	59.36	57.51	43.96	49.76	66.04	56.25	60.62
	GTS ‡	55.93	47.52	51.38	70.79	61.71	65.94	60.09	53.57	56.64	62.63	66.98	64.73
Ours	56.77	48.06	52.05	68.55	65.79	67.15	65.02	54.43	59.26	67.25	67.51	67.38	
BERT	JET _t ‡	51.48	42.65	46.65	70.20	53.02	60.41	62.14	47.25	53.68	71.12	57.20	63.41
	JET _o ‡	58.47	43.67	50.00	67.97	60.32	63.92	58.35	51.43	54.67	64.77	61.29	62.98
	GTS ‡	57.52	51.92	54.58	70.92	69.49	70.20	59.29	58.07	58.67	68.58	66.60	67.58
	[13] †	-	-	57.83	-	-	70.01	-	-	58.74	-	-	67.49
	Dual-MRC †	-	-	55.58	-	-	70.32	-	-	57.21	-	-	67.40
	Ours	62.71	54.53	58.33	77.03	67.46	71.92	64.62	60.62	62.55	68.45	70.61	69.51
BART	[14] †	-	-	57.59	-	-	72.46	-	-	60.11	-	-	69.98

(b) Results on ASTE-DATA-V2.

	Models	14Lap			14Rest			15Rest			16Rest		
		<i>P.</i>	<i>R.</i>	<i>F</i> ₁									
GloVe	CMLA+ ‡	30.09	36.92	33.16	39.19	47.13	42.79	34.56	39.84	37.01	41.34	42.10	41.72
	RINANTE+ ‡	21.71	18.66	20.07	31.42	39.38	34.95	29.88	30.06	29.97	25.68	22.30	23.87
	Li-unified-R ‡	40.56	44.28	42.34	41.04	67.35	51.00	44.72	51.39	47.82	37.33	54.51	44.31
	Peng20 ‡	37.38	50.38	42.87	43.24	63.66	51.46	48.07	57.51	52.32	46.96	64.24	54.21
	JET _t ‡	52.00	35.91	42.48	66.76	49.09	56.58	59.77	42.27	49.52	63.59	50.97	56.59
	JET _o ‡	53.03	33.89	41.35	61.50	55.13	58.14	64.37	44.33	52.50	70.94	57.00	63.21
	Ours	54.38	49.35	51.74	64.75	66.70	65.71	58.89	56.70	57.77	65.93	63.62	64.75
BERT	JET _t ‡	53.53	43.28	47.86	63.44	54.12	58.41	68.20	42.89	52.66	65.28	51.95	57.85
	JET _o ‡	55.39	47.33	51.04	70.56	55.94	62.40	64.45	51.96	57.53	70.40	58.37	63.83
	[15] †	57.84	59.33	58.58	63.59	73.44	68.16	54.53	63.30	58.59	63.57	71.98	67.52
	GTS †	58.54	50.65	54.30	67.25	69.22	68.22	60.69	60.54	60.61	67.39	66.73	67.06
	Ours	65.25	53.79	58.97	71.75	70.52	71.13	62.77	59.79	61.25	68.20	69.26	68.73
BART	[14] †	61.41	56.19	58.69	65.52	64.99	65.25	59.14	59.38	59.26	66.60	68.68	67.62

TABLE III: Main results on ASTE-DATA-V1 and ASTE-DATA-V2. ‘GloVe’, ‘BERT’ and ‘BART’ signify the pre-trained embedding or model used in different methods. The baseline results with ‡, †, *, †, †, † and † are from [3], [16], [17], [14], [5], [13] and [15], respectively. The best results on each dataset are in **boldface**.

C. Experimental Setup

For embedding layer, following [3], we use GloVe with dimension 300 or BERT-base-uncased⁴ without fine-tuning. For the sequence encoder, the hidden size d_h , the number of head h and layer L are set to 200, 8 and 3, respectively. For the table encoder, the dimension of cell vector, the hidden size of MDGRU and the layer number L are set to 200, 200 and 3, respectively. We use Adam [23] as our optimizer with inverse time learning rate decay, the decay rate is 0.05 and decay step is 1000, and the learning rate is set to 0.001. Dropout [24] is set to 0.5, and the batch size is 6. We select the model parameter with the best F1 on the valid dataset and apply it to the test data for evaluation. Details of all the hyper-parameters are provided in Table V.

D. Main Results

Table III reports the results of our model and baseline models. Firstly, when using GloVe, our model achieves the best results on all eight datasets. Secondly, when using contextual pre-trained model, our BERT-based model outperforms all previous BERT-based methods. Compared with [14], which uses BART pre-trained model, on the one hand, our BERT-based model achieves better results on six datasets, e.g., 5.88F1 points improvement on V2-14Rest, and only achieves slight lower results on two datasets, i.e., 0.54F1 points on V1-14Rest and 0.47F1 points on V1-16Rest. On the other hand, the pre-trained parameters of BART-base model used in [14] is 29M more than BERT-base parameters used in our model (nearly 30% parameters of BERT-base). Thirdly, our GloVe-based model even beats previous popular BERT-based models, e.g., JET, OTE. In conclusion, we provides a new state-of-the-art solution for ASTE, since we carefully design the combination

⁴<https://huggingface.co/bert-base-uncased/tree/main>

Models	14Lap			14Rest			15Rest			16Rest		
	<i>P.</i>	<i>R.</i>	<i>F</i> ₁									
Both	65.25	53.79	58.97	71.75	70.52	71.13	62.77	59.79	61.25	68.20	69.26	68.73
w/o SFI	62.78	51.76	56.74	70.98	68.41	69.67	64.07	57.73	60.74	66.10	67.51	66.79
w/o TGA	61.98	52.13	56.63	71.11	67.10	69.05	66.01	55.26	60.16	68.02	65.37	66.67
w/o Both	60.57	51.39	55.60	71.24	66.30	68.68	65.45	55.46	60.04	70.48	62.26	66.12

TABLE IV: The influence of the explicit interaction on ASTE-DATA-V2. Both denoted full model with both table guide attention (TGA) and sequence feature injection (SFI). w/o SFI, w/o TGA and w/o Both represent models without SFI, without TGA and without both of them, respectively.

#Layer	3
Dropout	0.5
Optimizer	Adam
Learning Rate	$1e-3$
Batch Size	6
Max Step	5000
GloVe Embedding Size	300
GRU Hidden Size d_h	200
#Attention Head	8
MDGRU Hidden Size d_h	200
Table Encoder Cell Size	200

TABLE V: Hyperparameters used in our experiments.

of subtasks, introduce a table encoder to extract compositional features of target-opinion pairs and strengthen the explicit interaction between subtasks.

V. ANALYSIS

A. Effect of Explicit Interactions

In ASTE, the interaction among different subtasks is important for three elements in the triplet are closely related. On top of implicit interaction, we introduce a bidirectional explicit interaction between two subtasks with table guide attention (TGA) and sequence feature injection (SFI). In this part, we explore the effect of TGA and SFI.

Firstly, we remove the TGA and SFI from the model in turn. Specifically, when removing TGA, we follow [25] and utilize the multi-head self-attention [26] to aggregate features in the sequence encoder. When removing SFI, we calculate the input for two MDGRUs with the output of the base encoder. As shown in Table IV, bidirectional explicit interaction model (Both) outperforms unidirectional explicit interaction models (w/o SFI and w/o TGA), in addition, w/o SFI and w/o TGA beat the model without explicit interaction (w/o Both). Secondly, we share the parameters of two encoders in different layers. When the number of layers in the model increases, as shown in Figure 6, the performance of the model without explicit interaction does not improve, however, the model with explicit interactions can benefit from the increasing layer number. Since the number of parameters remains unchanged when sharing parameters, we conclude that the model performance benefits from the explicit interactions. These results show the importance of the explicit interaction in ASTE.

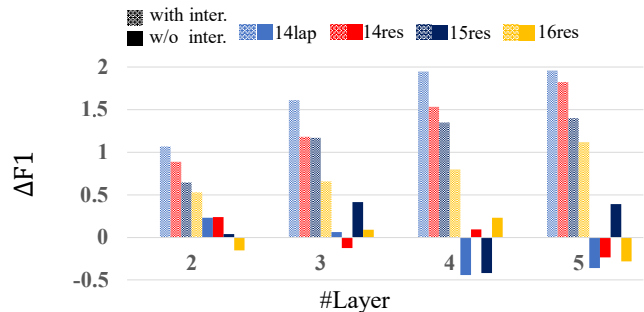


Fig. 6: Results on ASTE-DATA-V2. The model performance change when increasing number of layers in table-sequence encoders. Notably the model size remains unchanged as the parameters are shared across different layers. $\Delta F1$ is the absolutely F1 change over encoders with only *one* layer. [with inter] and [w/o inter] denote models with and without two explicit interactions, respectively.

	great	pizza	,	poor	service
great		POS _✓			
pizza	POS _✓				
,	Only	Seq.		Only	Tab.
poor		NEG _✗			NEG _✓
service	POS _✗			NEG _✓	

Fig. 7: A case study which shows the effectiveness of the table encoder. Model with only sequence encoder (below the diagonal line) wrongly matches ‘poor’ with ‘pizza’, ‘great’ with ‘service’. While table encoder correctly identifies paired targets and opinions.

B. Effect of Table Encoder

The table encoder explicitly injects the inductive bias of compositional token pair representation into model, so it can reduce the erroneous predictions on non-existent triplets. In this part, we explore the effect of the table encoder. Our table encoder, biaffine scorer [8] of OTE and GTS establish the similar tabular like structures. However, our table encoder extracts token-pair level features and the other two methods only model token level features. To better explore our table encoder’s advantage, we only use the sequence

Models	14Lap	14Rest	15Rest	16Rest
Both	58.97	71.13	61.25	68.73
OnlyTab	56.40	69.38	60.49	67.64
OnlySeq	50.95	60.21	54.96	59.76
GTS	54.30	68.22	60.61	67.06

TABLE VI: The F1 results of full model, models using only one encoder, GTS and [15] on four datasets of ASTE-DATA-V2.

	15Rest	16Rest	14Lap	14Rest
JET _o	57.53	63.83	51.04	62.40
Ours	61.25	68.73	58.97	71.13
Δ	+3.72	+4.90	+7.93	+8.73
$R_{t>1}$	34.67%	40.97%	44.07%	58.21%

TABLE VII: The performance gain on four datasets of ASTE-DATA-V2. Δ is the absolute F1 improvement, and $R_{t>1}$ represents the ratio of sentences with multiple triplets on each dataset.

encoder (OnlySeq) and the table encoder (OnlyTab) to solve ASTE separately. For OnlySeq, following OTE, we utilize biaffine scorer to establish the table for sentiment classification. For OnlyTab, we use the diagonal cells to detect targets and opinions.⁵

As shown in Table VI, OnlyTab outperforms OnlySeq (all 4 datasets) and GTS (3 out of 4 datasets), which shows the importance of compositional feature for ASTE. The performance of OnlyTab on 15Rest is slightly lower than that of GTS, we think the reason is that there are relatively small number of multiple triplets on 15Rest as shown in Table VII. In addition, we also conduct a case study to intuitively show the effect of our table encoder, as shown in Figure 7, the top-right and bottom-left triangles of the matrix represent the sentiment classification results of OnlyTab and OnlySeq, respectively. In this case, the sentence contains two opinions, *great* and *poor*, which express positive and negative sentiment. Since the sequence encoder extracts features at the token level, the sentiment of *great* and *poor* misleads the classification results, i.e., (*service*, POS, *great*) and (*pizza*, NEG, *poor*). However, the table encoder, which extracts sentiment features at the token-pair level, obtains the right results. These results show that modeling the compositional feature of target-opinion pair is important for ASTE, and the table encoder plays a vital role for this propose.

C. Effect of Task Combination

ASTE is a composite triplet extraction task, which consists of 3 atom subtasks, and a reasonable subtask combination is essential for ASTE. Although solving all of 3 atom subtasks by a single module, e.g., GTS, JET_o and JET_t can enhance the interaction of different subtasks, they also effect each others. As shown in Table VI. Our full model Both outperforms OnlyTab, which extracts targets, opinions and sentiment through

⁵We set the number of layers of OnlyTab and OnlySeq to 3 and 6, respectively, so these two models have about the same number of parameters.

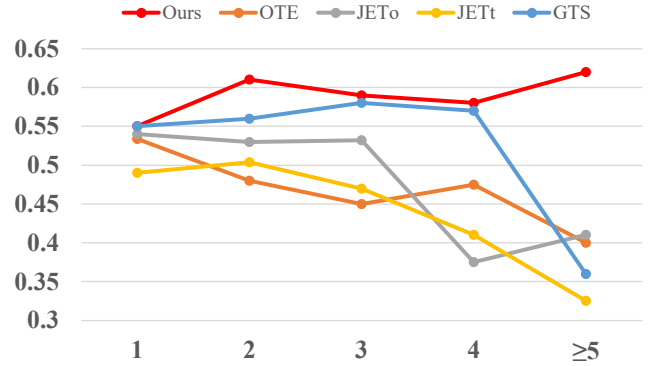


Fig. 8: Performances of different models in challenging situations in V2-14Lap dataset where multiple triplets exist.

sentence: it was pleasantly uncrowded , the service was delightful , the garden adorable , the food (from appetizers to entrees) was delectable				
Triplets	Golden	GTS	JET _o	Ours
(food, POS, delectable)	√	√		√
(garden, POS, adorable)	√	√	√	√
(service, POS, delightful)	√	√	√	√
(entrees, POS, delectable)	√	√	√	√
(appetizers, POS, delectable)	√	√		√
(service, POS, pleasantly)		√	√	
(service, POS, uncrowded)		√	√	

Fig. 9: A case study on a multiple-triplet sentence. The results of two representative baselines GTS, JET_o and our model.

a single module like GTS. We think enhancing the interaction of subtasks by explicit interaction mechanisms is better than formulate different subtasks as a unified task. Through explicit interaction, each module can utilize the useful information and drop the harmful information from other subtasks. However, when solving all subtasks through a single module, the single module must pay attention to all subtasks, so for a subtask, some harmful information from other subtasks can not be dropped optionally. Such a phenomenon of mutual interference is also found in other tasks [7], [42].

D. Performance in the Changeling Situation

Our model achieves noticeable performance gain over previous methods. In this part, we explore the advantage of our model. Firstly, compared with previous method JET, which has ill task formulation and extracts token-level feature, we find out that our model has advantage in dealing sentences with multiple triplets. As shown in Table VII, the situation that one sentence has multiple triplets is usual, e.g., such cases reach a ratio from 34.67% on 15Rest to 58.21% on 14Rest, and our model achieves more considerable performance gain on datasets with larger ratio $R_{t>1}$. We further divide the sentences according to the number of triplets in them. As shown in Figure 8, as the number of triplets in a sentence increases, our model outperforms other models more obviously. These results show that our model has more advantages over other methods in

handling such a changeling but common situation. We also conduct a case study to show this intuitively. The sentence in Figure 9 has 5 potential opinions (colored by green), 5 targets (colored by blue) and 5 golden triplets. Our model correctly extracts all triplets. However, JET_o misses two golden triplets of opinion *delectable* for its unreasonable subtask combination, and both JET_o and GTS extract two false triplets due to they are influenced by the potential opinion words with strong sentiment, e.g., *pleasantly* and *uncrowded*. We guess the performance gain in such a challenging situation benefits from our subtask combination, the explicit interaction mechanisms and the table encoder. Firstly, our subtask combination is more in line with human cognition, i.e., judging sentiment based on both target and opinion. Secondly, more triplets in one sentence cause the extraction more difficult, while our explicit interaction mechanisms can make different subtasks better promote each other, which helps the model perform stably. At last, since every target and every opinion may contain sentiment and form a triplet, more targets and opinions in one sentence will exacerbate the erroneous predictions on non-existent triplets, while our table encoder can alleviate this by extracting features at the token-pair level.

VI. CONCLUSION

In this paper, we divide ASTE into target-opinion detection and sentiment classification; then correspondingly utilize a sequence encoder and a table encoder to handle them. We establish bidirectional explicit interaction between two subtasks with table guide attention and sequence information injection. Besides, the table encoder extracts the compositional feature of target-opinion pairs by directly generating sentiment features at the token-pair level, which can reduce the erroneous predictions on non-existent triplets. Our method achieves the state-of-the-art performance on six popular ASTE datasets and has the advantage over previous models in the challenging but common situation where a sentence has multiple triplets.

REFERENCES

- [1] R. K. Bakshi, N. Kaur, R. Kaur, and G. Kaur, "Opinion mining and sentiment analysis," in *2016 3rd international conference on computing for sustainable global development (INDIACom)*. IEEE, 2016, pp. 452–455.
- [2] H. Peng, L. Xu, L. Bing, F. Huang, W. Lu, and L. Si, "Knowing what, how and why: A near complete solution for aspect-based sentiment analysis," in *AAAI*, 2020, pp. 8600–8607.
- [3] L. Xu, H. Li, W. Lu, and L. Bing, "Position-aware tagging for aspect sentiment triplet extraction," in *Proceedings of the 2020 Conference on Empirical Methods in Natural Language Processing (EMNLP)*, 2020, pp. 2339G–2349.
- [4] C. Zhang, Q. Li, D. Song, and B. Wang, "A multi-task learning framework for opinion triplet extraction," in *Proceedings of the 2020 Conference on Empirical Methods in Natural Language Processing: Findings*, 2020, pp. 819–828.
- [5] Z. Wu, C. Ying, F. Zhao, Z. Fan, X. Dai, and R. Xia, "Grid tagging scheme for aspect-oriented fine-grained opinion extraction," in *Findings of the Association for Computational Linguistics: EMNLP 2020*. Online: Association for Computational Linguistics, Nov. 2020, pp. 2576–2585. [Online]. Available: <https://www.aclweb.org/anthology/2020.findings-emnlp.234>
- [6] F. Li, Z. Wang, S. C. Hui, L. Liao, D. Song, J. Xu, G. He, and M. Jia, "Modularized interaction network for named entity recognition," in *Proceedings of the 59th Annual Meeting of the Association for Computational Linguistics and the 11th International Joint Conference on Natural Language Processing (Volume 1: Long Papers)*, 2021, pp. 200–209.
- [7] J. Wang and W. Lu, "Two are better than one: Joint entity and relation extraction with table-sequence encoders," in *Proceedings of the 2020 Conference on Empirical Methods in Natural Language Processing (EMNLP)*, 2020, pp. 1706–1721.
- [8] T. Dozat and C. D. Manning, "Deep biaffine attention for neural dependency parsing," *arXiv preprint arXiv:1611.01734*, 2016.
- [9] P. Gupta, H. Schütze, and B. Andrassy, "Table filling multi-task recurrent neural network for joint entity and relation extraction," in *Proceedings of COLING 2016, the 26th International Conference on Computational Linguistics: Technical Papers*, 2016, pp. 2537–2547.
- [10] M. Zhang, Y. Zhang, and G. Fu, "End-to-end neural relation extraction with global optimization," in *Proceedings of the 2017 Conference on Empirical Methods in Natural Language Processing*, 2017, pp. 1730–1740.
- [11] A. Graves, S. Fernández, and J. Schmidhuber, "Multi-dimensional recurrent neural networks," in *International conference on artificial neural networks*. Springer, 2007, pp. 549–558.
- [12] K. Cho, B. van Merriënboer, C. Gulcehre, D. Bahdanau, F. Bougares, H. Schwenk, and Y. Bengio, "Learning phrase representations using rnn encoder-decoder for statistical machine translation," in *Proceedings of the 2014 Conference on Empirical Methods in Natural Language Processing (EMNLP)*, 2014, pp. 1724–1734.
- [13] S. Chen, Y. Wang, J. Liu, and Y. Wang, "Bidirectional machine reading comprehension for aspect sentiment triplet extraction," *arXiv preprint arXiv:2103.07665*, 2021.
- [14] H. Yan, J. Dai, X. Qiu, Z. Zhang *et al.*, "A unified generative framework for aspect-based sentiment analysis," *arXiv preprint arXiv:2106.04300*, 2021.
- [15] L. Huang, P. Wang, S. Li, T. Liu, X. Zhang, Z. Cheng, D. Yin, and H. Wang, "First target and opinion then polarity: Enhancing target-opinion correlation for aspect sentiment triplet extraction," *arXiv preprint arXiv:2102.08549*, 2021.
- [16] Z. Chen, H. Huang, B. Liu, X. Shi, and H. Jin, "Semantic and syntactic enhanced aspect sentiment triplet extraction," *arXiv preprint arXiv:2106.03315*, 2021.
- [17] H. Yang, B. Zeng, J. Yang, Y. Song, and R. Xu, "A multi-task learning model for chinese-oriented aspect polarity classification and aspect term extraction," *Neurocomputing*, vol. 419, pp. 344–356, 2019.
- [18] W. Wang, S. J. Pan, D. Dahlmeier, and X. Xiao, "Coupled multi-layer attentions for co-extraction of aspect and opinion terms," in *Thirty-First AAAI Conference on Artificial Intelligence*, 2017.
- [19] H. Dai and Y. Song, "Neural aspect and opinion term extraction with mined rules as weak supervision," in *Proceedings of the 57th Annual Meeting of the Association for Computational Linguistics*, 2019, pp. 5268–5277.
- [20] X. Li, L. Bing, P. Li, and W. Lam, "A unified model for opinion target extraction and target sentiment prediction," in *Proceedings of the AAAI Conference on Artificial Intelligence*, vol. 33, 2019, pp. 6714–6721.
- [21] Y. Mao, Y. Shen, C. Yu, and L. Cai, "A joint training dual-mrc framework for aspect based sentiment analysis," *arXiv preprint arXiv:2101.00816*, 2021.
- [22] M. Lewis, Y. Liu, N. Goyal, M. Ghazvininejad, A. Mohamed, O. Levy, V. Stoyanov, and L. Zettlemoyer, "BART: Denoising sequence-to-sequence pre-training for natural language generation, translation, and comprehension," in *Proceedings of the 58th Annual Meeting of the Association for Computational Linguistics*. Online: Association for Computational Linguistics, Jul. 2020, pp. 7871–7880. [Online]. Available: <https://www.aclweb.org/anthology/2020.acl-main.703>
- [23] D. P. Kingma and J. Ba, "Adam: A method for stochastic optimization," *arXiv preprint arXiv:1412.6980*, 2014.
- [24] N. Srivastava, G. Hinton, A. Krizhevsky, I. Sutskever, and R. Salakhutdinov, "Dropout: a simple way to prevent neural networks from overfitting," *The journal of machine learning research*, vol. 15, no. 1, pp. 1929–1958, 2014.
- [25] Y. Song, J. Wang, T. Jiang, Z. Liu, and Y. Rao, "Attentional encoder network for targeted sentiment classification," *arXiv preprint arXiv:1902.09314*, 2019.
- [26] A. Vaswani, N. Shazeer, N. Parmar, J. Uszkoreit, L. Jones, A. N. Gomez, Ł. Kaiser, and I. Polosukhin, "Attention is all you need," in *Advances in neural information processing systems*, 2017, pp. 5998–6008.
- [27] A. Agarwal, B. Xie, I. Vovsha, O. Rambow, and R. J. Passonneau, "Sentiment analysis of twitter data," in *Proceedings of the workshop on language in social media (LSM 2011)*, 2011, pp. 30–38.
- [28] X. Fang and J. Zhan, "Sentiment analysis using product review data," *Journal of Big Data*, vol. 2, no. 1, p. 5, 2015.

- [29] Q. Le and T. Mikolov, "Distributed representations of sentences and documents," in *International conference on machine learning*. PMLR, 2014, pp. 1188–1196.
- [30] Z. Zhao, "Learning document embeddings by predicting n-grams for sentiment classification of long movie reviews," in *Workshop Contribution (ICLR)*, 2016.
- [31] T. Thongtan and T. Phienthrakul, "Sentiment classification using document embeddings trained with cosine similarity," in *Proceedings of the 57th Annual Meeting of the Association for Computational Linguistics: Student Research Workshop*, 2019, pp. 407–414.
- [32] L. Dong, F. Wei, C. Tan, D. Tang, M. Zhou, and K. Xu, "Adaptive recursive neural network for target-dependent twitter sentiment classification," in *Proceedings of the 52nd annual meeting of the association for computational linguistics (volume 2: Short papers)*, 2014, pp. 49–54.
- [33] A. Rietzler, S. Stabinger, P. Opitz, and S. Engl, "Adapt or get left behind: Domain adaptation through bert language model finetuning for aspect-target sentiment classification," in *Proceedings of The 12th Language Resources and Evaluation Conference*, 2020, pp. 4933–4941.
- [34] S. Manandhar, "Semeval-2014 task 4: aspect based sentiment analysis," in *Proceedings of the 8th international workshop on semantic evaluation (SemEval 2014)*, 2014.
- [35] P. Chen, Z. Sun, L. Bing, and W. Yang, "Recurrent attention network on memory for aspect sentiment analysis," in *Proceedings of the 2017 conference on empirical methods in natural language processing*, 2017, pp. 452–461.
- [36] L. Xu, L. Bing, W. Lu, and F. Huang, "Aspect sentiment classification with aspect-specific opinion spans," *arXiv preprint arXiv:2010.02696*, 2020.
- [37] D. Ma, S. Li, X. Zhang, and H. Wang, "Interactive attention networks for aspect-level sentiment classification," *arXiv preprint arXiv:1709.00893*, 2017.
- [38] B. Yang and C. Cardie, "Extracting opinion expressions with semi-markov conditional random fields," in *Proceedings of the 2012 Joint Conference on Empirical Methods in Natural Language Processing and Computational Natural Language Learning*, 2012, pp. 1335–1345.
- [39] X. Li, L. Bing, P. Li, W. Lam, and Z. Yang, "Aspect term extraction with history attention and selective transformation," in *Proceedings of the 27th International Joint Conference on Artificial Intelligence*, 2018, pp. 4194–4200.
- [40] D. Ma, S. Li, and H. Wang, "Joint learning for targeted sentiment analysis," in *Proceedings of the 2018 Conference on Empirical Methods in Natural Language Processing*, 2018, pp. 4737–4742.
- [41] E. Ekinici and S. İlhan Omurca, "An aspect-sentiment pair extraction approach based on latent dirichlet allocation for turkish," *International Journal of Intelligent Systems and Applications in Engineering*, vol. 6, no. 3, pp. 209–213, 2018.
- [42] Z. Zhong and D. Chen, "A frustratingly easy approach for joint entity and relation extraction," *arXiv preprint arXiv:2010.12812*, 2020.
- [43] T. Nayak and H. T. Ng, "Effective modeling of encoder-decoder architecture for joint entity and relation extraction," in *Proceedings of the AAAI Conference on Artificial Intelligence*, vol. 34, no. 05, 2020, pp. 8528–8535.
- [44] S. Xiao, M. Song *et al.*, "A text-generated method to joint extraction of entities and relations," *Applied Sciences*, vol. 9, no. 18, p. 3795, 2019.
- [45] D. Sui, Y. Chen, K. Liu, J. Zhao, X. Zeng, and S. Liu, "Joint entity and relation extraction with set prediction networks," *arXiv preprint arXiv:2011.01675*, 2020.